NIH Public Access
Author Manuscript
DNA Repair (Amst). Author manuscript; available in PMC 2009 August 2.

Published in final edited form as:
DNA Repair (Amst). 2008 August 2; 7(8): 1298–1308.

The histone methylase Set2p and the histone deacetylase Rpd3p repress meiotic recombination at the *HIS4* meiotic recombination hotspot in *Saccharomyces cerevisiae*

Jason D. Merker[a,b], **Margaret Dominska**[c], **Patricia W. Greenwell**[c], **Erica Rinella**[a], **David C Bouck**[a], **Yoichiro Shibata**[d], **Brian D. Strahl**[d], **Piotr Mieczkowski**[c], and **Thomas D. Petes**[c,*]

a *Department of Biology, University of North Carolina, Chapel Hill, NC 27599-3280*

c *Department of Molecular Genetics and Microbiology, Duke University Medical Center, Durham, NC 27710-3054*

d *Department of Biochemistry and Biophysics University of North Carolina School of Medicine Chapel Hill, NC 27599*

Abstract

The rate of meiotic recombination in the yeast *Saccharomyces cerevisiae* varies widely in different regions of the genome with some genes having very high levels of recombination (hotspots). A variety of experiments done in yeast suggest that hotspots are a feature of chromatin structure rather than a feature of primary DNA sequence. We examined the effects of mutating a variety of enzymes that affect chromatin structure on the recombination activity of the well-characterized *HIS4* hotspot including the Set2p and Dot1p histone methylases, the Hda1p and Rpd3p histone deacetylases, the Sin4p global transcription regulator, and a deletion of one of the two copies of the genes encoding histone H3–H4. Loss of Set2p or Rpd3p substantially elevated *HIS4* hotspot activity, and loss of Hda1p had a smaller stimulatory effect; none of the other alterations had a significant effect. The increase of *HIS4* hotspot activity in *set2* and *rpd3* strains is likely to be related to the recent finding that histone H3 methylation by Set2p directs deacetylation of histones by Rpd3p.

2. Introduction

The rate of meiotic recombination varies considerably at different positions in the yeast genome (1,2). This variation reflects differences in the frequency of local meiosis-specific double-strand DNA breaks (DSBs), the recombination-initiating lesion (3,4) catalyzed by Spo11p and associated proteins (5). There are several lines of evidence that the frequency of DSBs is regulated by elements of chromatin structure rather than primary DNA sequence (2). First, recombination hotspots exhibit hypersensitivity to nucleases (6–10). Some loci (8,9) undergo meiosis-specific alterations in nuclease sensitivity prior to DSB formation, although no such changes are observed at other loci (6). Since all nuclease-hypersensitive regions are not meiotic

*Corresponding author: Department of Molecular Genetics and Microbiology, Duke University, Medical Center, Durham, NC 27710-3054; phone: (919) 684-4986; FAX (919) 684-6033; email: tom.petes@duke.edu.
b Current address: Department of Pathology, Stanford University Medical Center, Stanford, CA 94305-5324

Publisher's Disclaimer: This is a PDF file of an unedited manuscript that has been accepted for publication. As a service to our customers we are providing this early version of the manuscript. The manuscript will undergo copyediting, typesetting, and review of the resulting proof before it is published in its final citable form. Please note that during the production process errors may be discovered which could affect the content, and all legal disclaimers that apply to the journal pertain.

Conflicts of interest
None.

NIH-PA Author Manuscript
NIH-PA Author Manuscript
NIH-PA Author Manuscript

NIH-PA Author Manuscript

NIH-PA Author Manuscript

NIH-PA Author Manuscript

recombination hotspots (6,10), “open” chromatin appears necessary, but not sufficient, for meiotic recombination hotspot activity. Second, insertion of a nucleosome-excluding sequence into the yeast genome creates a recombination hotspot (11). Third, the activity of some hotspots requires the binding of transcription factors, but not high levels of transcription (2). This result has been interpreted as indicating that chromatin modifications associated with transcription factor binding stimulate both transcription and recombination. Finally, some mutants that affect chromatin modifications reduce the frequency of meiosis-specific DSBs. In the yeast *S. pombe*, mutations in a histone acetylase or in a chromatin-remodeling activity reduce the activity of the *ade6-M26* recombination hotspot (12). In *S. cerevisiae*, loss of Set1p (a histone methyltransferase) or Rad6p (a ubiquitin-conjugating enzyme) reduce DSB formation (13, 14).

In our genetic background, the *HIS4* gene is one of the strongest recombination hotspots in the *S. cerevisiae* genome (15) and is associated with a high-frequency DSB located upstream of *HIS4* (16,17). In cells sporulated at 25°, this DSB is responsible for initiating about half of *HIS4* conversion events (16). The binding of four transcription factors (Bas1p, Bas2p, Rap1p, and Gcn4p) is required for optimal levels of this DSB (16,18–20). One role of these transcription factors is presumably to recruit chromatin-modifying complexes to the *HIS4* promoter. The transcription factor Rap1p directly alters the positioning of nucleosomes in the *HIS4* upstream region (21,22). Based on the evidence that *HIS4* hotspot activity is likely related to a particular chromatin structure, in this study, we analyzed the effects of mutations affecting chromatin modifications on *HIS4* hotspot activity.

Two broad classes of protein complexes maintain or alter local chromatin structure: proteins that mediate post-translational modification of histones and other chromatin-related proteins, and ATP-dependent nucleosome remodeling complexes (23). The amino-terminal ‘tails’ of histones are subject to various covalent modifications including acetylation, methylation, phosphorylation, ubiquitination, and ADP-ribosylation (24). These modifications affect chromatin structure by altering histone-DNA or histone-histone contacts (25), and/or by collectively establishing a code that is recognized by downstream effector proteins and complexes (24). The chromatin-modifying activities are recruited to certain loci by sequence-specific transcription factors (26,27), or by association with RNA polymerase II (27,28).

Since there are many proteins involved in modifying chromatin, our analysis emphasized mutants that were reported to affect the expression of *HIS4* or to alter its chromatin structure. Mutations in *RPD3*, encoding an H4 histone deacetylase (26), were reported to reduce *HIS4* expression about three-fold in one study (29), although no significant change was observed in another study (30). Deletion of the *HDA1*-encoded histone H3 and H2B deacetylase (31), resulted in a three-fold increase of *HIS4* gene expression in one study (30), but had no significant effect on expression in another study (29). The deletion of *SIN4*, a transcription factor that is part of the Mediator complex, reduced *HIS4* transcription about 15-fold and altered *HIS4* chromatin structure (32). In addition, Wyrick *et al.* (33) found that depletion of histone H4 decreased *HIS4* expression two-fold.

In addition to examining these mutants previously demonstrated to affect *HIS4* expression, we analyzed the effects of several other related mutants. We examined mutants of *SET2* (encoding an H3K36 histone methylase, 34), since it has been recently reported (35–37) that Set2p-dependent methylation recruits an Rpd3p-containing repressive complex (Rpd3C[S]). We also examined the effects of eliminating Dot1p, an H3K79 histone methyltransferase (38,39). H3K79 methylation is at low levels at yeast telomeres (40), but occurs at high levels at actively-transcribed genes (41). As described below, we found that deletion of *SET2* or *RPD3* strongly stimulated *HIS4* hotspot activity, whereas deletion of *HDA1* had a more subtle stimulatory effect. None of the other mutants examined had any significant effect. We also showed that

NIH-PA Author Manuscript

NIH-PA Author Manuscript

NIH-PA Author Manuscript

strains that lacked either *SET2* or *RPD3* had elevated levels of H3K27 acetylation near the *HIS4* recombination hotspot in meiosis, and elevated meiotic *HIS4* gene expression.

2. Materials and methods

2.1. Yeast strains

All strains used were derived by transformation from the haploid strains AS4 (*∝trp1 arg4 tyr7 ade6 ura3*) and AS13 (*a leu2 ura3 ade6 rme1*) (42). Derivatives of AS4 and AS13 are listed in Table 1; diploids constructed by crossing AS4 and AS13 derivatives are described in Table 2. Deletions were constructed by replacing the relevant gene with a *kanMX4* cassette (43) or *hphMX4* cassette (44), which contain a gene that confers geneticin or hygromycin resistance, respectively. The PCR synthesis of the cassettes and subsequent transformation were performed as described by Wach *et al.* (43), using the plasmid pFA6-kanMX4 (*kanMX4* cassette; 43) or pAG32 (*hphMX4* cassette; 44) and the primer pairs listed in Table 3. One pair of *set2::hphMX4* strains, ER4 and ER5, had complete deletions of *SET2* and was constructed with primers *set2Δ*-F and *set2Δ*-R. A second pair of strains, DCB4 and DCB6, had a substitution that deleted the last 100 amino acids of the Set2p (*set2::kanMX4*). In all the assays in our study, these two types of *set2* mutations had the same phenotypes. All constructions, unless noted otherwise, were checked by PCR. The *rad50S* derivatives were constructed as described by Alani *et al.* (45).

2.2. Genetic analysis

Standard materials and methods were used (46) except where noted. Diploids were sporulated on plates at 25°C. Although the *HIS4* hotspot is stronger at 18°C (16), not all of the mutants sporulated at this temperature. Following tetrad dissection on plates with rich growth medium (YPD), the spore colonies were replica-plated to various omission media; spore colonies on medium lacking histidine were examined microscopically in order to detect small sectors.

2.3. Southern analysis

Cells were harvested from *rad50S* diploid strains just prior to being placed on a sporulation plate (0 hr) or after 24 hr at 25° C. Cells were washed with 0.5 ml 10 mM Tris (pH 8.0)-1 mM EDTA, and stored at −80° C. DNA isolation and Southern blot procedures were performed as described by Nag and Petes (17). The *HIS4* DSB was examined using a *Bgl*II digest, and an *Xho*I-*Bgl*II fragment of *HIS4* derived from pDN42 as a hybridization probe (17). The *ARG4* DSB was examined using a *Bgl*II digest, and an *Eco*RV-*Bgl*II fragment derived from pAK1 as a hybridization probe (16). Hybridization was quantitated using a PhosphorImager (Molecular Dynamics), and the percent of molecules with a DSB was calculated as described by Kirkpatrick *et al.* (47). Since the percentage of molecules that receive a DSB is affected by the sporulation efficiency, the percentage of DSBs at *HIS4* was normalized to the percentage of DSBs at *ARG4*.

We also did Southern analysis of intact chromosomal DNA molecules. For these experiments, DNA molecules were separated using CHEF (contour-clamped homogeneous electric field) gel electrophoresis as described previously (48). DNA was isolated from cells immediately after transfer to solid sporulation medium or after 24 hours in solid sporulation medium (room temperature, 23°–25° C). Following electrophoresis, DNA was transferred to a Nylon membrane and hybridized to a probe derived from left end of chromosome III, within the *CHA1* gene. The probe was generated by PCR amplification of yeast genomic DNA with the primers ChrIII-15830 and ChrIII-16773 (Table 3).

NIH-PA Author Manuscript

NIH-PA Author Manuscript

NIH-PA Author Manuscript

2.4. Analysis of histone modifications using chromatin immunoprecipitation (ChIP)

Cell extracts were prepared from the diploid strains used for ChIP analysis (FX1, JDM1093, JDM1095, and JDM1096) as described by Xiao *et al.* (49). Prior to extraction, the cells were incubated on solid sporulation medium for six hours at room temperature (23°–25° C.). Cells at this time point are beginning to form DSBs and binucleate cells appear at about 10 hours (17). Immunoprecipitation of formaldehyde-fixed chromatin was done with the following antibodies: anti-H3K36me3 (AB9050, Abcam), anti-H3K27ac (07–360, Upstate), and anti-H3 (AB1791, Abcam). Following the immunoprecipitation, we reversed the crosslinks by treatment of the samples at 65° C and performed multiplex PCR to amplify sequences in the *HIS4* and *BIK1* region.

Four sets of primers were used (sequences in Table 3). A PCR reaction with primers BIK1codpre350F and BIK1codpre350R results in a 350 bp fragment (termed "A") derived from the 5′ end of *BIK1*. The 300 bp "B" fragment (located at the 3′ end of *BIK1*) and the 242 bp "C" fragment (located in the intergenic region upstream of *HIS4*) flank the site of the DSB associated with the *HIS4* hotspot. The primers used to produce the "B" and "C" fragments are BIK1codpost300F and BIK1codpost300R, and HIS4pro242F and HIS4pro242R, respectively. The fourth primer pair, which generates the 180 bp "D" fragment are HIS4codpost180F and HIS4codpost180R. The "D" sequences are derived from the 3′ end of *HIS4*. We also utilized primers (IntergenicV-1 and IntergenicV-2) to amplify a control locus on chromosome V that was used in previous studies (49); this region has a low intrinsic level of histone methylation. The multiplex procedure involved using all five pairs of primers (four from the *HIS4-BIK1* region and the control pair) in one reaction. The products of the PCR reaction were analyzed on 12% polyacrylamide gels that were stained with ethidium bromide. The number of pixils in each band was measured using the Kodak 100 Imaging System.

The levels of histone modifications for the four fragments near the *HIS4* recombination hotspot were calculated as a ratio (*a/b*) as described previously (49). The *a* value is also a ratio: (*w/x)/(y/z*), where *w* is the amount of the PCR fragment from the *HIS4* region in the ChIP sample, *x* is the amount of control PCR fragment in the ChIP sample, *y* is the amount of PCR fragment from the *HIS4* region in the input DNA, and *z* is the amount of PCR fragment from the control locus in the input DNA. The *b* values were calculated similarly using the data obtained with antibodies directed against H3 histone; the *b* values are used to control for histone occupancy at each site. At least three independent experiments were done for each strain. For each experiment, we calculated separately the (*a/b*) ratio and the ratios were averaged. In summary, we calculate the level of histone modifications in the *HIS4* region relative to a locus on chromosome V and corrected for the level of histone occupancy at each position.

2.5. Analysis of meiotic expression of *HIS4* and *BIK1*

We examined the meiotic mRNA levels of *HIS4* and *BIK1* in cells harvested after six hours incubation in sporulation medium at 23° C. RNA was isolated using the Yeast RNA Kit (Omega Biotech) and these RNA samples were reverse-transcribed into DNA using the High Capacity cDNA Reverse Transcription Kit (Applied Biosystems) according to the instructions of the manufacturer. The real-time PCR was performed with the *Power* SYBR Green PCR Master Mix (Applied Biosystems) using the Applied Biosystems Step One Plus PCR machine. After a 10 minute 95°C "start-up" incubation, we used 40 cycles of PCR with the following temperatures and step times: 95° C, 15 seconds; 60° C, 1 minute.

Three sets of primers were used for this analysis. The pairs of primers used to monitor the *HIS4* and *BIK1* cDNAs were his4_185_U and his4_185_L, and BIK1-388-F and BIK1-531-R, respectively (Table 3). We measured the cDNA levels of the control *RNA1* gene with primers RNA1_128_U and RNA1_128_L. The *RNA1* gene was chosen as a control because its mRNA

NIH-PA Author Manuscript

NIH-PA Author Manuscript

NIH-PA Author Manuscript

level is not affected by sporulation (50) or by the *rpd3* mutation (29,30). In our analysis, we first normalized the levels of *BIK1* and *HIS4* cDNAs to the level of *RNA1* cDNA. We subsequently normalized the levels of *BIK1* and *HIS4* cDNAs to the level of *HIS4* cDNA in the wild-type strain.

2.6. Data analysis

Statistical analysis was performed using Instat 1.12 (GraphPad Software) for the Macintosh. The Fisher's exact test with a two-tailed P value or Chi-squared analysis (for comparisons that involve more than two experimental measures) were used for all comparisons, and $P<0.05$ was considered statistically significant. For the ChIP experiments, standard errors of the mean were calculated using Excel.

3. Results

We used two different assays to monitor the effects of mutations affecting chromatin structure on the recombination activity of the *HIS4* hotspot. First, we monitored the rate of aberrant segregation of a heterozygous *HIS4* marker in the wild-type strain and strains homozygous for various mutations. Second, for some strains, we examined the rate of meiosis-specific double-strand DNA breaks (DSBs) at the *HIS4* and *ARG4* loci. In our previous studies (16) and those of others (51), these two assays for recombination activity generally yield the same result.

3.1. Tetrad analysis of strains with mutations affecting chromatin structure

When a yeast strain that is heterozygous for alleles *A* and *a* undergoes meiosis, most tetrads segregate 2*A*:2*a* spores (Mendelian segregation). There are two classes of aberrant segregation events, gene conversion and postmeiotic segregation (PMS) events. In most models of recombination (52), both gene conversion and PMS events reflect heteroduplex formation involving the heterozygous site, followed by mismatch repair (gene conversion) or failure to repair (PMS events). Thus, the frequency of aberrant segregation tetrads is a measurement of the rate of local recombination events. Although the average rates of conversion for markers in most genomic regions are low (less than 5% of the tetrads), the rates of conversion for markers at the *HIS4* and *ARG4* loci in our genetic background are very high. At the *HIS4* locus, more than 50% of the tetrads have aberrant segregation when the cells are sporulated at 18°C. (16). When the cells are sporulated at 25° C., the rate of aberrant segregation is approximately halved. In the experiments described below, we used the higher temperature of sporulation because the *set2* strains failed to sporulate at 18° C.

Our analysis is summarized in Table 4. The *set2* mutation in two closely-related genetic backgrounds resulted in a very significant ($p < 0.0001$) stimulation of the rate of aberrant segregation for the *HIS4*, but not the *ARG4*, marker. Since the rate of aberrant segregation is much higher for *HIS4* than *ARG4* (which affects the power of the statistical test), we cannot rule out the possibility that both loci are affected by the *set2* mutation to similar extents; this possibility, however, is excluded by the physical analysis of DSBs described in Section 3.2. The wild-type strain DNY11 is isogenic (except for the *set2* mutation) with ER6 and the wild-type strain DNY26 strain is isogenic with DCB9. We observed a significant increase in crossing over in the *HIS4-LEU2* interval for the DNY26/DCB9 comparison, although the increase for the DNY11/ER6 comparison was not significant. We also found that a mutation of the Hda1p deacetylase significantly stimulated the rate of aberrant segregation of the *HIS4* marker, although the magnitude of this stimulation was half of that observed for the *set2* mutation. Loss of the Dot1p methylase, the Sin4p transcription factor, and loss of one copy of the H3-H4 histone pair had no effect on the hotspot activity associated with the *HIS4* gene.

NIH-PA Author Manuscript

NIH-PA Author Manuscript

NIH-PA Author Manuscript

As described in the Introduction, Set2p-dependent methylation of H3K36 is involved in the recruitment of the histone deacetylase Rpd3p. Thus, one explanation of the effects of the *set2* mutation is that loss of the Set2p-dependent recruitment of Rpd3p results in hyper-acetylated chromatin that allows more efficient entry of the Spo11p recombination machinery and, therefore, more DSBs in the *HIS4* region. This model predicts that loss of Rpd3p would also result in a higher level of aberrant segregation. We could not check this prediction by tetrad analysis, since (as reported previously, 53) *rpd3* mutants did not complete meiosis and failed to produce viable spores. An adjustment of the sporulation conditions that allowed *rpd3* mutants to complete sporulation in some genetic backgrounds (54) did not allow sporulation in our genetic background. To confirm our conclusions about the effects of the *set2* mutation on recombination and to examine the effect of *rpd3* mutants on *HIS4* recombination activity, we measured the rate of meiosis-specific DSBs at *HIS4* in wild-type, *set2*, *rpd3*, and *set2 rpd3* double mutant strains.

3.2. Measurement of meiosis-specific DSBs at the *HIS4* and *ARG4* loci in wild-type, *set2*, *rpd3*, and *set2 rpd3* diploid strains

Since meiotic recombination is initiated by a DSB (3,4), the frequency of local DSBs measured by Southern analysis is a direct measurement of recombination activity. We constructed derivatives of the wild-type, *set2*, *rpd3*, and *set2 rpd3* diploids (Table 2) that were homozygous for the *rad50S* mutation, which prevents subsequent processing of DSBs (45). These strains were sporulated at 25° C., and DSBs were examined at both the *HIS4* and *ARG4* loci. The Southern analysis for one set of experiments in which we examined DSBs at the *HIS4* locus is shown in Fig. 1. Since the efficiency of cells undergoing meiotic DSB formation can vary from one experiment to another, we normalized the levels of DSBs measured at the *HIS4* locus to the levels observed at the *ARG4* locus (as described in Materials and Methods). Normalizing the ratio of *HIS4* to *ARG4* DSBs to 1 for the wild-type strains FX1 and FX3, we found this ratio averaged 3.3 for the *set2* strains JDM1093 and DCB16, 2.7 for the *rpd3* strain JDM1095, and 4.1 for the *set2 rpd3* strain JDM1096. We also examined the % DSBs relative to the unbroken parental fragments for *HIS4* and *ARG4*. These values are somewhat more variable than the normalized *HIS4/ARG4* ratio, since the fraction of cells in sporulation medium that undergo DSB formation is somewhat variable from culture to culture. The % DSBs for *HIS4* and *ARG4*, respectively, in the various strains were: 4.5, 2.6 (FX1, wild-type); 3.0, 0.6 (FX3, wild-type), 12.9, 2.7 (JDM1093, *set2*); 8.3, 0.4 (DCB16, *set2*); 19.1, 3.9 (JDM1095, *rpd3*); 18, 2.1 (JDM1096, *set2 rpd3*). These values represent the average of two independent experiments for each strain, except for FX3 and DCB16 which represent a single experiment. Although our analysis does not rule out the possibility that *set2* and *rpd3* mutations stimulate DSB formation at *ARG4*, the degree of stimulation is clearly stronger at *HIS4*.

These results confirm the conclusion, based on tetrad analysis, that the *set2* mutation elevates recombination rates at the *HIS4* hotspot. This elevation does not reflect the presence of novel DSBs near *HIS4*, but the strengthening of the same DSB site observed in the wild-type strain (Fig. 1A). The *set2* and *rpd3* mutations had similar effects on the frequency of *HIS4*-associated DSBs, and the *set2 rpd3* double mutant strain had an effect that was only slightly stronger than the single mutants. This result suggests that Set2p and Rpd3p may be acting in the same pathway to stimulate *HIS4* hotspot activity. It should be noted that the increase in DSB formation observed in the mutant strains is substantially greater than the increase in gene conversion rates. In part, this difference is attributable to the observation that only half of the conversion events at *HIS4* in cells sporulated at 25° are a consequence of the DSB site shown in Fig. 1A (16).

We also examined DSBs on chromosome III by Southern analysis of chromosomal DNA molecules separated by CHEF (contour-clamped homogeneous electric field) gel

NIH-PA Author Manuscript

NIH-PA Author Manuscript

NIH-PA Author Manuscript

electrophoresis (Fig. 1B). As observed previously (55), DSBs on chromosome III occurred in two clusters, one on the left arm (which includes the *HIS4* DSB) and one on the right arm. From the analysis shown in Fig. 1B, it is clear that mutations in *set2* and *rpd3* substantially elevated the DSB frequency of the *HIS4* hotspot relative to other DSBs on chromosome III. In Fig. 1B, DSBs on the right arm of III appear to be repressed in strains with the *set2* and *rpd3* mutations. It is possible that strengthening of the *HIS4* DSB reduces the frequency of DSBs on the same chromosome; we and others have previously observed local competition between DSB sites. Alternatively, it is possible that Rpd3p- and Set2p-mediated modifications repress meiotic recombination at some loci and stimulate recombination at others.

3.3. Histone modifications near the *HIS4* hotspot in wild-type, *set2*, *rpd3*, and *set2 rpd3* strains

Loss of the Rpd3p deacetylase results in increased acetylation of many sites in H3 and H4 histones (56,57), whereas loss of the Set2p methylase directly affects only methylation of H3K36 (34). The Set2p-mediated methylation, however, helps recruit a repressive Rpd3p-containing complex to chromatin, and elevated histone acetylation was observed for several loci in *set2* mutant strains (35,37). Consequently, we examined the histone acetylation levels at H3K27 by chromatin immunoprecipitation (ChIP analysis) in the diploids FX1 (wild-type), JDM1093 (*set2*), JDM1095 (*rpd3*), and JDM1096 (*set2 rpd3*). For this analysis, chromatin was isolated from cells sporulated for six hours, about the time of DSB formation (17). We used four different PCR products (labeled A–D in Fig. 2A) to look at H3K27 acetylation levels at four sites in the *HIS4* region. The A fragment (located near the 5′ end of *BIK1*) and the D fragment (located near the 3′ end of *HIS4*) are more than 1 kb from the site of the DSB. The B and C fragments are within about 200 bp of the DSB site. ChIP experiments were done with antibodies directed against acetylation of H3K27, and unmodified histone H3 (as a histone occupancy control). In addition, we used an antibody directed against tri-methylation of H3K36 in extracts derived from the wild-type, *rpd3*, and *set2* strains.

The ChIP data were normalized in two ways: by comparison to a control DNA fragment (an intergenic region on chromosome V) and by comparison to the level of nucleosome occupancy (monitored using an antibody directed against histone H3); details of these normalizations are described in Materials and Methods. We found that the regions near the DSB sites were hyper-acetylated at the H3K27 sites in the *set2*, *rpd3*, and *set2 rpd3* strains (Fig. 2B). The acetylation was elevated most strongly for the sites (B and C fragments) located near the site of the DSB. As expected, the region near the DSB site had lower nucleosome occupancy than the regions represented by the A and D fragments (Fig. 2C). Finally, we found that the tri-methylation of H3K36 was not substantially affected in *rpd3* strains, but was, as expected, eliminated in the *set2* strain (Fig. 2D). The interpretation of these results will be described below.

3.4. Meiotic expression of *HIS4* and *BIK1* is elevated in strains with *set2* or *rpd3* mutations

Although there is not a direct relationship between gene expression and the level of meiotic recombination (2), some mutations reduce both gene expression and meiotic recombination. For example, at *HIS4*, deletion of the Bas2p transcription factor binding site, which reduces the level of *HIS4* expression, also substantially reduces the *HIS4* recombination hotspot activity (19). Consequently, we used real-time PCR to measure the level of *BIK1* and *HIS4* mRNA in wild-type, *set2*, *rpd3*, and *set2 rpd3* strains incubated for six hours in sporulation medium. As shown in Fig. 3, expression levels for both genes (*BIK1* levels shown by white bars, *HIS4* by stippled bars) were significantly elevated in the mutant strains relative to the wild-type strain. These results indicate that the chromatin alterations associated with the *rpd3* and *set2* mutations at the *HIS4* locus elevate both meiotic recombination and meiotic gene expression.

NIH-PA Author Manuscript

NIH-PA Author Manuscript

NIH-PA Author Manuscript

4. Discussion

The main conclusions from our study are: 1) loss of the Set2 and Rpd3 proteins strongly elevates *HIS4* hotspot activity, whereas loss of the Hda1p has a weaker stimulating effect, and 2) loss of the Dot1 and Sin4 protein, or a reduction in the amount of histones H3 and H4 do not affect *HIS4* hotspot activity. These results will be discussed further below.

Since mutations in *SET2* and *RPD3* stimulate meiosis-specific DSBs at the *HIS4* hotspot to approximately the same extent and since the double mutant strain has a level of DSBs that is not substantially greater than the single mutants, we favor the possibility that Set2p and Rpd3p act in the same pathway to repress hotspot activity. Similarly, the *BIK1* expression level is elevated to about the same extent in the double mutant compared to both single mutants, although *HIS4* expression is somewhat greater in the double mutant than in either single mutant (Fig. 3). Based on the recent evidence that Set2p-mediated methylation of H3K36 is involved in the recruitment of a repressive Rpd3 complex (35–37), the simplest explanation of these observations is that this complex negatively regulates both meiotic recombination and transcription. This negative regulation is likely to be a consequence of a closed chromatin structure caused by Rpd3p-mediated deacetylation. Our chromatin immunoprecipitation experiments, although limited in scope, are also consistent with this possibility. We found that acetylation of H3K27 was elevated in the *set2*, *rpd3*, and *set2 rpd3* strains near the site of the *HIS4* DSB in meiotic cells. These results suggest that the elevated recombination at *HIS4* reflects a more open chromatin structure resulting from increased acetylation of histones.

There are a number of caveats concerning this explanation. In our study, as in most studies of the effects of chromatin-modifying enzymes, it is difficult to distinguish direct from indirect effects. For example, microarray analysis indicates *rpd3Δ* affects the expression of over 400 genes (29) and one of these gene products could indirectly stimulate meiotic recombination. Although we cannot exclude indirect effects of the *set2* and *rpd3* mutations, a number of arguments suggest that the effects at the *HIS4* hotspot may be direct, in addition to the ChIP data discussed above. First, Robyr *et al*. (58) found that the level of histone H4K12 acetylation (a modification regulated by Rpd3p; 57) in the region adjacent to the *HIS4* DSB site is increased approximately three-fold in an *rpd3Δ* strain relative to wild type. Second, Kurdistani *et al*. (59) found that Rpd3p binds in the *HIS4* intergenic region. Third, in our study, the *set2* and *rpd3* mutations differentially affect the rate of meiotic recombination at *HIS4* and *ARG4*. The frequency of DSB formation in the *rpd3* and *set2* mutants is clearly more elevated at *HIS4* than at *ARG4*. In addition, the frequency of DSBs at *HIS4* is elevated relative to many other DSB sites on chromosome III (Fig. 1B). Thus, our results are unlikely to be explained by the argument that the elevated level of *HIS4* recombination reflects increased expression of Spo11p and other components of the meiotic recombination machinery in *rpd3* and *set2* strains.

Our observation that meiotic expression of *HIS4* is somewhat elevated in *rpd3* and *set2* strains contrasts with the observation that the level of *HIS4* gene expression is reduced by the *rpd3* mutation (29), although no such reduction was observed in another study (30). These differences may reflect differences in the pattern of mitotic and meiotic expression and/or strain differences. We also found that the *hda1* mutation significantly elevated the activity of the *HIS4* hotspot (Table 4), although this effect was smaller than that observed for the *set2* and *rpd3* mutations. Since the Hda1p histone deacetylase has somewhat different activities than the Rpd3p deacetylase (56), this result may argue that the general level of histone acetylation is more important in regulating *HIS4* hotspot activity than a specific type of modification. Although we cannot rule out an indirect effect of *hda1* on recombination, *HIS4* gene expression is elevated about three-fold by the *hda1* mutation in one study (30), although no effect on expression was found in another study (29).

NIH-PA Author Manuscript

NIH-PA Author Manuscript

NIH-PA Author Manuscript

As described in the Introduction, many mutations that reduce *HIS4* transcription (deletion of transcription factors or their binding sites upstream of *HIS4*) also reduce *HIS4* meiotic recombination (11,18–20,47). White *et al*. (60) showed, however, that deletion of the TATAA sequence upstream of *HIS4* significantly decreased *HIS4* expression, but had no effect on meiotic recombination. In this study, we found that the *sin4* deletion, which reduces *HIS4* expression about 15-fold (32), had no effect on *HIS4* hotspot activity. Similarly, a reduction in the level of histones H3 and H4 that stimulates *HIS4* gene expression had no effect on *HIS4* hotspot activity. These results support our earlier conclusion that, although some features of chromatin structure favor both gene expression and recombination, other features may specifically stimulate one process or the other.

Whatever the precise mechanism responsible for the elevated recombination in the *set2* and *rpd3* strains, our results demonstrate that the activity of one of the strongest hotspots in the genome can be further elevated. In an analysis of the *ade6-M26* hotspot in *S. pombe*, Yamada *et al*. (12) reported that loss of the SpGcn5 histone acetylase or deletion of the Snf22 histone-remodeling proteins reduced the activity of the hotspot. Since the loss of a histone acetylase would be expected to decrease acetylation at the *ade6-M26* hotspot, the mechanism by which loss of SpGcn5 reduces hotspot activity may be related to the mechanism by which loss of Set2p, Rpd3p, and Hda1p stimulate hotspot activity.

Acknowledgements

We thank J. Lieb for discussions concerning chromatin structure. This research was supported by National Institutes of Health grants GM24110 (TDP) and GM68088 (BDS). B. D. Strahl is a Pew Scholar in the Biomedical Sciences.

References

1. Lichten M, Goldman ASH. Meiotic recombination hotspots. Ann Rev Genet 1995;29:423–444. [PubMed: 8825482]
2. Petes TD. Meiotic recombination hot spots and cold spots. Nature 2001;2:360–369.
3. Sun H, Treco D, Schultes NP, Szostak JW. Double strand breaks at an initiation site for meiotic gene conversion. Nature 1989;338:87–90. [PubMed: 2645528]
4. Szostak JW, Orr-Weaver TL, Rothstein R, Stahl FW. The double-strand-break repair model for recombination. Cell 1983;33:25–35. [PubMed: 6380756]
5. Keeney S, Giroux CN, Kleckner N. Meiosis-specific DNA double-strand breaks are catalyzed by Spo11, a member of a widely conserved protein family. Cell 1997;88:375–384. [PubMed: 9039264]
6. Fan QQ, Petes TD. Relationship between nuclease-hypersensitive sites and meiotic recombination hot spot activity at the *HIS4* locus of *Saccharomyces cerevisiae*. Mol Cell Biol 1996;16:2037–2043. [PubMed: 8628269]
7. Keeney S, Kleckner N. Communication between homologous chromosomes: genetic alterations at a nuclease-hypersensitivity site can alter meiotic chromatin structure at that site both in *cis* and in *trans*. Genes Cells 1996;1:475–489. [PubMed: 9078379]
8. Mizuno K, Emura Y, Baur M, Kohli J, Ohta K, et al. The meiotic recombination hotspot created by the single-base substitution *ade6-M26* results in remodeling of chromatin structure in fission yeast. Genes Dev 1997;11:876–886. [PubMed: 9106659]
9. Ohta K, Shibata T, Nicolas A. Changes in chromatin structure at recombination initiation sites during yeast meiosis. EMBO J 1994;13:5754–5763. [PubMed: 7988571]
10. Wu TC, Lichten M. Meiosis-induced double-strand breaks determined by yeast chromatin structure. Science 1994;263:515–518. [PubMed: 8290959]
11. Kirkpatrick DT, Wang YH, Dominska M, Griffith JD, Petes TD. Control of meiotic recombination and gene expression in yeast by a simple repetitive DNA sequence that excludes nucleosomes. Mol Cell Biol 1999;19:7661–7671. [PubMed: 10523654]

NIH-PA Author Manuscript

NIH-PA Author Manuscript

NIH-PA Author Manuscript

12. Yamada T, Mizuno K, Hirota K, Kon N, Wahls WP, et al. Roles of histone acetylation and chromatin remodeling factor in a meiotic recombination hotspot. EMBO J 2004;23:1792–1803. [PubMed: 14988732]

13. Sollier J, Lin W, Soustelle C, Suhre K, Nicolas A, et al. Set1 is required for meiotic S-phase onset, double-strand break formation and middle gene expression. EMBO J 2004;23:1957–1967. [PubMed: 15071505]

14. Yamashita K, Shinohara M, Shinohara A. Rad6-Bre1-mediated histone H2B ubiquitylation modulates the formation of double-strand breaks during meiosis. Proc Natl Acad Sci USA 2004;101:11380–11385. [PubMed: 15280549]

15. Gerton J, Derisi J, Shroff R, Lichten M, Brown PO, et al. Global mapping of meiotic recombination hotspots and coldspots in the yeast *Saccharomyces cerevisiae*. Proc Natl Acad Sci USA 2000;97:11383–11390. [PubMed: 11027339]

16. Fan QQ, Xu F, Petes TD. Meiosis-specific double-strand DNA breaks at the *HIS4* recombination hot spot in the yeast *Saccharomyces cerevisiae*: control in *cis* and *trans*. Mol Cell Biol 1995;15:1679–1688. [PubMed: 7862159]

17. Nag DK, Petes TD. Physical detection of heteroduplexes during meiotic recombination in the yeast *Saccharomyces cerevisiae*. Mol Cell Biol 1993;13:2324–2331. [PubMed: 8455614]

18. Abdullah MFF, Borts RH. Meiotic recombination frequencies are affected by nutritional states in *Saccharomyces cerevisiae*. Proc Natl Acad Sci USA 2001;98:14524–14529. [PubMed: 11724920]

19. White MA, Dominska M, Petes TD. Transcription factors are required for the meiotic recombination hotspot at the *HIS4* locus in *Saccharomyces cerevisiae*. Proc Natl Acad Sci USA 1993;90:6621–6625. [PubMed: 8341678]

20. White MA, Wierdl M, Detloff P, Petes TD. DNA-binding protein RAP1 stimulates meiotic recombination at the *HIS4* locus in yeast. Proc Natl Acad Sci USA 1991;88:9755–9759. [PubMed: 1946399]

21. Devlin C, Tice-Baldwin K, Shore D, Arndt K. RAP1 is required for BAS1/BAS2- and GCN4-dependent transcription for the yeast *HIS4* gene. Mol Cell Biol 1991;11:3642–3651. [PubMed: 1904543]

22. Yu L, Morse RH. Chromatin opening and transactivator potentiation by RAP1 in *Saccharomyces cerevisiae*. Mol Cell Biol 1999;19:5279–5288. [PubMed: 10409719]

23. Workman JL, Kingston RE. Alteration of nucleosome structure as a mechanism of transcriptional activation. Annu Rev Biochem 1998;67:545–579. [PubMed: 9759497]

24. Strahl BD, Allis CD. The language of covalent histone modifications. Nature 2000;403:41–45. [PubMed: 10638745]

25. Hansen JC, Tse C, Wolffe AP. Structure and function of the core histone N-termini: more than meets the eye. Biochemistry 1998;37:17637–17641. [PubMed: 9922128]

26. Kadosh D, Struhl K. Targeted recruitment of the Sin3-Rpd3 histone deacetylase complex generates a highly localized domain of repressed chromatin *in vivo*. Mol Cell Biol 1998;18:5121–5127. [PubMed: 9710596]

27. Vignali M, Hassan AH, Neely KE, Workman JL. ATP-dependent chromatin remodeling complexes. Mol Cell Biol 2000;20:1899–1910. [PubMed: 10688638]

28. Xiao T, Hall H, Kizer KO, Shibata Y, Hall MC, et al. Phosphorylation of RNA polymerase II CTD regulates H3 methylation in yeast. Genes Dev 2003;17:1–10. [PubMed: 12514094]

29. Bernstein BE, Tong JK, Schreiber SL. Genomewide studies of histone deacetylase function in yeast. Proc Natl Acad Sci USA 2000;97:13708–13713. [PubMed: 11095743]

30. Hughes TR, Marton MJ, Jones AR, Roberts CJ, Stoughton R, et al. Functional discovery via a compendium of expression profiles. Cell 2000;102:109–126. [PubMed: 10929718]

31. Wu J, Carmen AA, Kobayashi R, Suka N, Grunstein M. HDA2 and HDA3 are related proteins that interact with and are essential for the activity of the yeast histone deacetylase HDA1. Proc Natl Acad Sci USA 2001;98:4391–4396. [PubMed: 11287668]

32. Jiang YW, Stillman DJ. Regulation of *HIS4* expression by the *Saccharomyces cerevisiae SIN4* transcriptional regulator. Genetics 1995;140:103–114. [PubMed: 7635278]

NIH-PA Author Manuscript

NIH-PA Author Manuscript

NIH-PA Author Manuscript

33. Wyrick JJ, Holstege FCP, Jennings EG, Causton HC, Shore D, et al. Chromosomal landscape of nucleosome-dependent gene expression and silencing in yeast. Nature 1999;402:418–421. [PubMed: 10586882]
34. Strahl BD, Grant PA, Briggs SD, Sun ZW, Bone JR, et al. Set2 is a nucleosomal histone H3-selective methyltransferase that mediates transcriptional repression. Mol Cell Biol 2002;22:1298–1306. [PubMed: 11839797]
35. Carrozza MJ, Li B, Florens L, Suganua T, Swanson SK, et al. Histone H3 methylation by Set2 directs deacetylation of coding regions by Rpd3S to suppress spurious transcription. Cell 2005;123:581–592. [PubMed: 16286007]
36. Joshi AA, Struhl K. Eaf3 chromodomain interaction with methylated H3-K36 links histone deacetylation to Pol II elongation. Mol Cell 2005;20:971–978. [PubMed: 16364921]
37. Keogh MC, Kurdistani SK, Morris SA, Ahn SH, Podolny V, et al. Cotranscriptional Set2 methylation of histone H3 Lysine 36 recruits a repressive Rpd3 complex. Cell 2005;123:593–605. [PubMed: 16286008]
38. Feng Q, Wang H, Ng HH, Erdjument H, Tempst P, et al. Methylation of H3-lysine 79 is mediated by a new family of HMTases without a SET domain. Curr Biol 2002;12:1052–1058. [PubMed: 12123582]
39. Ng HH, Feng Q, Wang H, Erdjument-Bromage H, Tempst P, et al. Lysine methylation within the globular domain of histone H3 by Dot1 is important for telomeric silencing and Sir protein association. Genes Dev 2002;16:1518–1527. [PubMed: 12080090]
40. Ng HH, Ciccone DN, Morshead KB, Oettinger MA, Struhl K. Lysine-79 of histone H3 is hypomethylated at silenced loci in yeast and mammalian cells: a potential mechanism for position-effect variegation. Proc Natl Acad Sci USA 2003;100:1820–1825. [PubMed: 12574507]
41. Pokholok DK, Harbison CT, Levine S, Cole M, Hannett NM, et al. Genome-wide map of nucleosome acetylation and methylation in yeast. Cell 2005;122:517–527. [PubMed: 16122420]
42. Stapleton A, Petes TD. The Tn3 beta-lactamase gene acts as a hotspot for meiotic recombination in yeast. Genetics 1991;127:39–51. [PubMed: 1849855]
43. Wach AA, Brachat A, Pohlmann R, Philippsen P. New heterologous modules for classical or PCR-based gene disruptions in *Saccharomyces cerevisiae*. Yeast 1994;10:1793–808. [PubMed: 7747518]
44. Goldstein AL, McCusker JH. Three new dominant drug resistance cassettes for gene disruption in *Saccharomyces cerevisiae*. Yeast 1999;15:1541–1553. [PubMed: 10514571]
45. Alani E, Padmore R, Kleckner N. Analysis of wild-type and *rad50* mutants of yeast suggests an intimate relationship between meiotic chromosome synapsis and recombination. Cell 1990;61:419–436. [PubMed: 2185891]
46. Sherman, F.; Fink, GR.; Hicks, JB. Methods in Yeast Genetics. Cold Spring Harbor Laboratory; Cold Spring Harbor, NY: 1983.
47. Kirkpatrick DT, Fan QQ, Petes TD. Maximal stimulation of meiotic recombination by a yeast transcription factor requires the transcription activation domain and a DNA binding domain. Genetics 1999;152:101–115. [PubMed: 10224246]
48. Lobachev KS, Gordenin DA, Resnick MA. The Mre11 complex is required for repair of hairpin-capped double-strand breaks and prevention of chromosome rearrangements. Cell 2002;108:183–193. [PubMed: 11832209]
49. Xiao T, Shibata Y, Rao B, Laribee RN, O'Rourke R, et al. The RNA polymerase II kinase Ctk1 regulates positioning of a 5′ histone methylation boundary along genes. Mol Cell Biol 2007;27:721–731. [PubMed: 17088384]
50. Chu S, DeRisi J, Eisen M, Mulholland J, Botstein D, Brown PO, et al. The transcriptional program of sporulation in budding yeast. Science 1998;282:699–705. [PubMed: 9784122]
51. Paques F, Haber JE. Multiple pathways of recombination induced by double-strand breaks in *Saccharomyces cerevisiae*. Microbiol Mol Biol Rev 1999;63:349–404. [PubMed: 10357855]
52. Petes, TD.; Malone, RE.; Symington, LS. Recombination in Yeast. In: Broach, J.; Jones, E.; Pringle, J., editors. The Molecular and Cellular Biology of the Yeast Saccharomyces: Genome Dynamics, Protein Synthesis, and Energetics. Cold Spring Harbor Laboratory Press; Cold Spring Harbor, NY: 1991. p. 407-521.

NIH-PA Author Manuscript

NIH-PA Author Manuscript

NIH-PA Author Manuscript

53. Dora EG, Rudin N, Martell JR, Esposito MS, Ramirez RM. *RPD3 (REC3)* mutations affect mitotic recombination in *Saccharomyces cerevisiae*. Curr Genet 1999;35:68–76. [PubMed: 10079324]
54. Burgess SM, Ajimura M, Kleckner N. *GCN5*-dependent histone H3 acetylation and *RPD3*-dependent histone H4 deacetylation have distinct, opposing effects on *IME2* transcription, during meiosis and during vegetative growth in budding yeast. Proc Natl Acad Sci USA 1999;96:6835–6840. [PubMed: 10359799]
55. Zenvirth D, Arbel T, Sherman A, Goldway M, Klein S, et al. Multiple sites for double-strand breaks in whole meiotic chromosomes of *Saccharomyces cerevisiae*. EMBO J 1992;11:3441–3447. [PubMed: 1324174]
56. Rundlett SE, Carmen AA, Kobayashi R, Bavykin S, Turner BM, et al. *HDA1* and *RPD3* are members of distinct yeast histone deacetylase complexes that regulate silencing and transcription. Proc Natl Acad Sci USA 1996;93:14503–14508. [PubMed: 8962081]
57. Suka N, Suka Y, Carmen AA, Wu J, Grunstein M. New antibodies for sites of acetylation determine novel histone site usage in heterochromatin and euchromatin. Mol Cell 2001;8:473–479. [PubMed: 11545749]
58. Robyr D, Suka Y, Xenarios I, Kurdistani SK, Wang A, et al. Microarray deacetylation maps determine genome-wide functions for yeast histone deacetylases. Cell 2002;109:437–446. [PubMed: 12086601]
59. Kurdistani SK, Robyr D, Tavazoie S, Grunstein M. Genome-wide binding map of the histone deacetylase Rpd3 in yeast. Nat Genet 2002;31:248–254. [PubMed: 12089521]
60. White MA, Detloff P, Strand M, Petes TD. A promoter deletion reduces the rate of mitotic, but not meiotic, recombination at the *HIS4* locus in yeast. Curr Genet 1992;21:109–116. [PubMed: 1568254]
61. Nag DK, White MA, Petes TD. Palindromic sequences in heteroduplex DNA inhibit mismatch repair in yeast. Nature 1989;340:318–320. [PubMed: 2546083]
62. Benjamini Y, Hochberg Y. Controlling the false discovery rate: a practical and powerful approach to multiple testing. J R Stat Soc 1995;57:289–300.
63. Perkins DD. Biochemical mutants in the smut fungus *Ustilago maydis*. Genetics 1949;34:607–626.

NIH-PA Author Manuscript
NIH-PA Author Manuscript
NIH-PA Author Manuscript

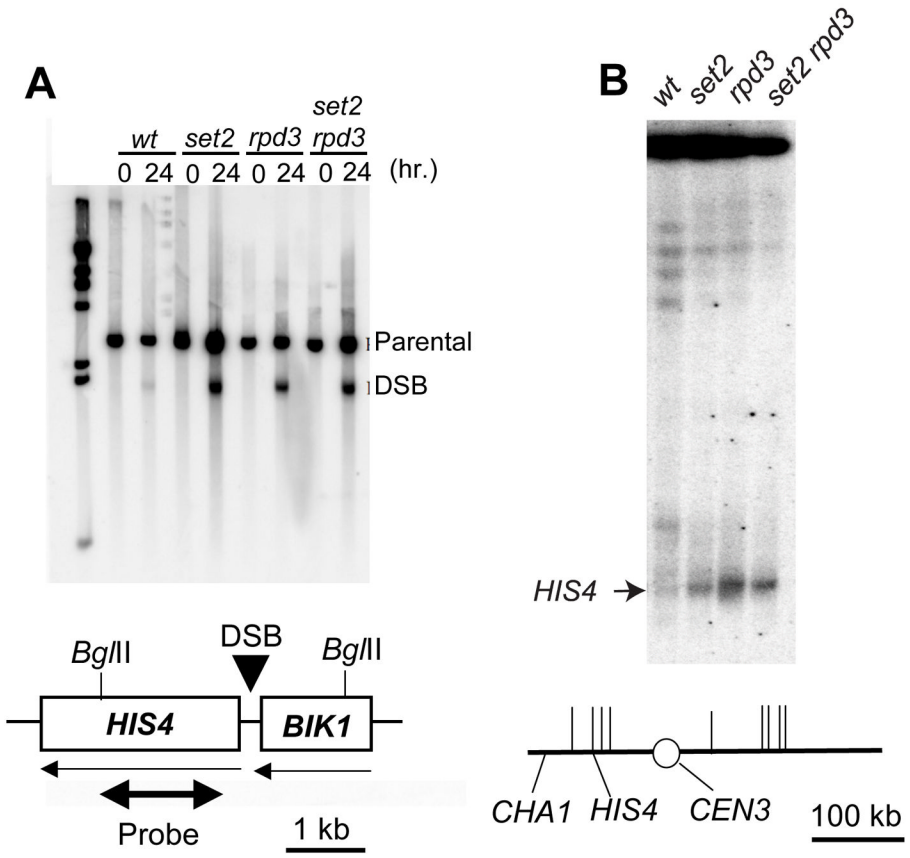

Figure 1. Southern analysis of *HIS4* meiosis-specific DSBs in chromatin structure mutants

DNA was isolated from cells just prior to (0 hr) and after a 24 hr (Fig. 1A) or 48 h (Fig. 1B) incubation period on solid sporulation medium. Samples were examined by standard gel electrophoresis (Fig. 1A) or CHEF gel electrophoresis (Fig. 1B).

A. The DNA was digested with BglII, and examined by Southern analysis using a *Xho*I-*Bgl*II fragment of *HIS4* as a hybridization probe (shown as a double-headed arrow in the lower part of the figure). The parental band (at roughly 3 kb) represents the unbroken *Bgl*II fragments, while the DSB band (at roughly 1.9 kb) represents fragments with a meiosis-specific DSB at *HIS4*. All strains are homozygous for the *rad50S* mutation. FX1 has no mutations in genes affecting chromatin structure. JDM1093, JDM1095, and JDM1096 are isogenic derivatives of FX1 homozygous for *set2Δ*, *rpd3Δ*, and *set2Δ rpd3Δ* mutations, respectively. In the schematic, horizontal arrows indicate the direction of transcription and the vertical arrow shows the DSB site associated with the *HIS4* hotspot.

B. For CHEF gel electrophoresis, DNA was prepared and the resulting molecules separated by electrophoresis using the methods described by Lobachev *et al.* (48). Following electrophoresis, the chromosomal DNA molecules were transferred to a Nylon membrane and hybridized to *CHA1* sequences, a gene located near the left end of chromosome III. The band of hybridization near the top of the gel represents chromosome III molecules without a DSB. The chromosomal DNA with a DSB at the *HIS4* hotspot is shown with an arrow. Chromosome III is depicted in the lower part of the figure. The short vertical lines represent the positions of meiotic recombination hotspots determined by microarray analysis (15).

NIH-PA Author Manuscript

NIH-PA Author Manuscript

NIH-PA Author Manuscript

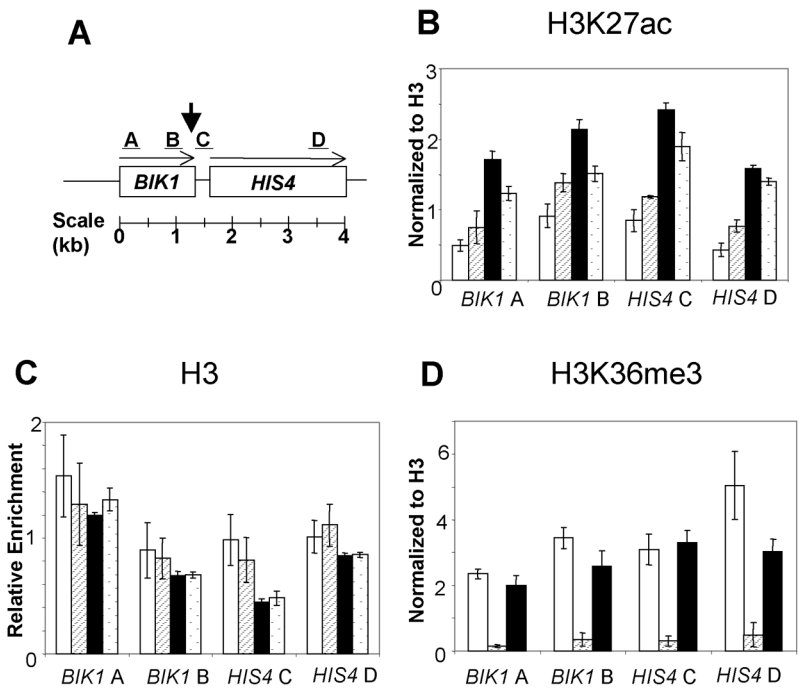

Figure 2. Chromatin modifications near the *HIS4* hotspot examined by chromatin immunoprecipitation

Cell extracts were prepared from the same diploid strains that were analyzed for DSBs: FX1 (wild-type, white bars), JDM1093 (*set2*, striped bars), JDM1095 (*rpd3*, black bars), and JDM1096 (*set2 rpd3*, stippled bars). The levels of histone modifications for four different fragments (A–D, Fig. 2A) were monitored by multiplex PCR. The arrow in Fig. 2A shows the approximate location of the recombination-associated DSB. Antibodies against H3K27 acetylation (panel B), histone H3 (panel C), or H3K36 tri-methylation (panel D) were used to precipitate chromatin harvested from meiotic cells incubated for six hours in sporulation medium. As described in the Materials and Methods, the levels of acetylation and methylation were normalized to a control region on chromosome V. In addition, the levels of acetylation and methylation were normalized for histone occupancy, using the data derived from the immunoprecipitations shown in Fig. 2C. Error bars represent the standard error of the mean.

NIH-PA Author Manuscript

NIH-PA Author Manuscript

NIH-PA Author Manuscript

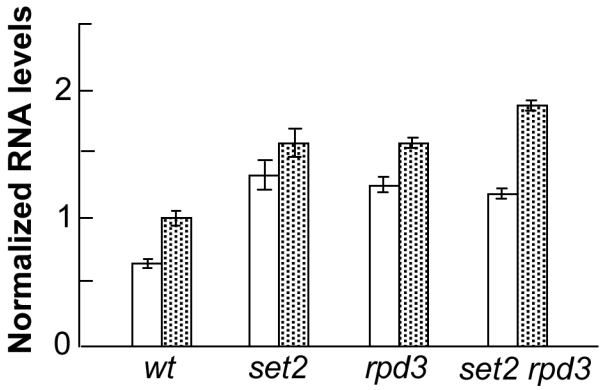

Figure 3. Meiotic gene expression of *HIS4* and *BIK1* in wild-type, *set2*, *rpd3*, and *set2 rpd3* strains

RNA was isolated from wild-type (FX1), *set2* (JDM1093), *rpd3* (JDM1095), and *set2 rpd3* strains that had been incubated for six hours in sporulation medium. Following reverse transcription of the RNA, we measured the levels of the resulting *BIK1* (shown by the white bars) and *HIS4* (shown by the stippled bars) cDNAs by real-time PCR (details in Materials and Methods). Following normalization of the amounts to the level of *RNA1* (a gene whose expression is unaffected by *set2* or *rpd3* mutations), the expression levels were normalized to the level of *HIS4* expression in the wild-type strain. Bars represent 95% confidence limits.

NIH-PA Author Manuscript
NIH-PA Author Manuscript
NIH-PA Author Manuscript

Table 1

Genotypes of haploid yeast strains

Strain	Relevant genotype; reference	Name of *rad50S* derivative; reference
	AS4-derived haploids	
AS4	WT; 43	DNY107; 16
ER4	*set2::hphMX4*	JDM205
DCB4	*set2::kanMX4*	DCB14
MD136	*rpd3::kanMX4*	JDM210
ER2	*dot1::hphMX4*	
JDM166	*hda1::kanMX4*	
MD131	*hht2-hhf2::kanMX4*	
MD133	*sin4::kanMX4*	
JDM214	*set2::hphMX4 rpd3::kanMX4 rad50S*	JDM214
	AS13-derived haploids	
AS13	WT; 42	
DNY9	*his4-lop*; 16	HF1; 16
DNY25	*his4-lopc*; 16	HF4; 16
ER5	*his4-lop set2::hphMX4*	JDM204
DCB6	*his4-lopc set2::kanMX4*	DCB15
MD135	*his4-lop rpd3::kanMX4*	JDM131
ER1	*his4-lop dot1::hphMX4*	
MD141	*his4-lop hda1::kanMX4*	
MD132	*his4-lop hht2-hhf2::kanMX4*	
MD134	*his4-lop sin4::kanMX4*	
JDM213	*his4-lop set2::hphMX4 rpd3::kanMX4 rad50S*	JDM213

All haploid strains were derived from AS4 (*α arg4-17 trp1 tyr7-1 ade6 ura3*) and AS13 (*a leu2 ade6 ura3 rme1*) by transformation or by crosses with isogenic strains. The mutant *his4-lop* and *his4-lopc* are 26 bp palindromic insertions that result in inefficiently-repaired mismatches (61). Only those markers that are different from the haploid progenitor strains are shown. If no reference is given, the strains were constructed in this study.

NIH-PA Author Manuscript
NIH-PA Author Manuscript
NIH-PA Author Manuscript

Table 2

Diploid yeast strains used in this study

Strain	Relevant homozygous mutations	Cross; reference[a]
	Strains heterozygous for *his4-lop*	
DNY11	WT	AS4 X DNY9; 16
FX1	*rad50S::URA3*	DNY107 X HF1; 16
ER6	*set2::hphMX4*	ER4 X ER5
JDM1093	*set2::hphMX4 rad50S::URA3*	JDM205 X JDM204
JDM1094	*rpd3::kanMX4*	MD136 X MD135
JDM1095	*rpd3::kanMX4 rad50S::URA3*	JDM210 X JDM131
ER3	*dot1::hphMX4*	ER2 X ER1
JDM1076	*hda1::kanMX4*	JDM166 X MD141
MD137	*hht2-hhf2::kanMX4*	MD131 X MD132
MD138	*sin4::kanMX4*	MD133 X MD134
JDM1096	*set2::hphMX4 rpd3::kanMX4 rad50S::URA3*	JDM214 X JDM213
	Strains heterozygous for *his4-lopc*	
DNY26	WT	AS4 X DNY25; 16
FX3	*rad50S::URA3*	DNY107 X HF4; 16
DCB9	*set2::kanMX*	DCB4 X DCB6
DCB16	*set2::kanMX rad50S::URA3*	DCB14 X DCB15

[a] Genotypes of the haploids used in the constructions are given in Table 1. In crosses, AS4- and AS13-derived strains are shown on the left and the right of the X, respectively.

DNA Repair (Amst). Author manuscript; available in PMC 2009 August 2.

NIH-PA Author Manuscript NIH-PA Author Manuscript NIH-PA Author Manuscript

Table 3

Primers used to make deletions with *kanMX4* or *hphMX4* cassettes[a] and for other types of analysis.

Primer name	Sequence (5′-3′)
set2Δ-F	**AGTCGTGCTGTCAAACCTTTCTCCTTTCCTGGTTGTTGTTTTACGTGATC**CGTACGCTGCAGGTCGAC
set2Δ-R	**CTTTGGGACAGAAAACGTGAAACAAGCCCCAAATATGCATGTCTGGTTAA**ATCGATGAATTCGAGCTCG
Set2 del UP	**TCACATTACCTATCATTACAGTGCTACTGATAGCCCACTAATGCGGATAT**CGTACGCTGCAGGTCGAC
Set2 del DN	**TCTCCCAGTCCCAAAGACTAGAGCACAACTGGAATAAATTCTTTGCATCT**ATCGATGAATTCGAGCTCG
rpd3Δ-F	**TGCGCCATACAAAACATTCGTGGCTACAACTCGATATCCGTGCAG**CGTACGCTGCAGGTCGAC
rpd3Δ-R	**TTGTTTCACATTATTTATATTCGTATATACTTCCAACTCTTTTTT**ATCGATGAATTCGAGCTC
dot1Δ-F	**AAGGAGGTCACCAGTAATTGTGCGCTTTGGTTACATTTTGTTGTACAGTA**CGTACGCTGCAGGTCGAC
dot1Δ-R	**TATTTCTACTTAGTTATTCATACTCATCGTTAAAAGCCGTTCAAAGTGCC**ATCGATGAATTCGAGCTCG
hda1Δ-F	**GAGAAAGGGAAAGTTGAGCACTGTAATACGCCGAACAGATTAAGC**CGTACGCTGCAGGTCGAC
hda1Δ-R	**GGCATGAAGGTTGCCGAAAAAAAATTATTAATGGCCAGTTTTTCC**ATCGATGAATTCGAGCTC
hht2-hhf2Δ-F	**CCCCCAGTCTAAATGCATAGAAAAAAAAAAATTCCCGCTTTATAT**CGTACGCTGCAGGTCGAC
hht2-hhf2Δ-R[b]	**GGCATGAAAATAATTTCAACACCGATTGTTTAACCACCGATTGTT**ATCGATGAATTCGAGCTCG
sin4Δ-F	**AGAAAAGAAACTAGCAGACCTGACCTTCTGTTGGTAAATATTAGT**CGTACGCTGCAGGTCGAC
sin4Δ-R	**ATGTTTAAAACAATTCTATACAAAACTATGCTATAGTACTAATAA**ATCGATGAATTCGAGCTCG
BIK1codpre350F	GGATAGATATCAAAGAAAGATAGGATGTTTC
BIK1codpre350R	GGGATTTAGGATCATCCATGGG
BIK1codpost300F	GGTGCCAACGAAGATGTCG
BIK1codpost300R	GAAAATTGGCAACGATTCCAC
HIS4pro242F	GGCAGTCGAACTGACTCTAATAGTG
HIS4pro242R	CTATTGTATTACTATTACACAGCGCAG
HIS4codpost180F	CGTGTGGATATTGTTCGTAAATG
HIS4codpost180R	GTAAGCACCCACAAATACGGAC
IntergenicV-1	GGCTGTCAGAATATGGGGCCGTAGTA
IntergenicV-2	CACCCCGAAGCTGCTTTCACAATAC
ChrIII-15830	CTGGAAATATGAAATTGTCAGCGAC
ChrIII-16773	TGAATGCCTTCAACCAAGTGGCTCCTTC
his4_185_U	CGTTGCTGCTATGGCTTACG
his4_185_L	CCACATCGGCATCTTCATCG
BIK1-388-F	CACAGCGGTAATCAACAGTC
BIK1-531-R	GCTGGTGGTGTTGTGATTAG
RNA1_128_U	CTGCTGGTTCAGATGAAGTC
RNA1_128_L	TTCCATAGCCGGTAAGAAGG

[a] Gene deletions were made using PCR fragments containing a selectable marker flanked by sequences from the gene to be deleted (43,44). For most of these constructions, the sequences of the oligonucleotides match those located immediately upstream and downstream of the gene to be deleted. The only exceptions are the Set2 del UP and Set2 del DN oligonucleotides. Set2 DN UP is located within *SET2*, about 300 bp from the end of the gene, and Set2p UP is located about 150 bp downstream of *SET2*. Sequences homologous to the region flanking the target gene are shown in bold-face type. Sequences homologous to the selectable cassette used to make the disruption are shown in regular type. The primers labeled “BIK1”, “HIS4”, and “Intergenic” were used in chromatin immunoprecipitation experiments.

[b] The primer *hht2-hhf2Δ*-R is missing a single base relative to the region downstream of *HHF2*, which creates a single base pair deletion when the PCR fragment is inserted in the locus. The correct sequence is GGCATGAAAATAATTTCAAACACCGATTGTTTAACCACCGATTGTT, with the deleted base underlined.

DNA Repair (Amst). Author manuscript; available in PMC 2009 August 2.

NIH-PA Author Manuscript
NIH-PA Author Manuscript
NIH-PA Author Manuscript

Table 4

Rates of meiotic recombination (aberrant segregation and crossovers) in strains with mutations affecting chromatin structure

Strain	Relevant genotype	# Tetrads	*HIS4* Ab. Seg. (%)	*ARG4* Ab. seg. (%)	*HIS4-LEU2* map dist. (cM)[c]
DNY11[a]	wild-type	475	25	6	24
DNY26[a]	wild-type	515	27	6	24
ER6	*set2::hphMX4*	647	38[b]	8	26
DCB9	*set2::kanMX4*	556	40[b]	7	30[c]
ER3	*dot1::hphMX4*	250	26	4	19
JDM1076	*hda1::kanMX4*	537	33[b]	9	25
MD137	*hht2-hhf2::kanMX4*	115	23	12	24
MD138	*sin4::kanMX4*	109	25	6	19

[a]The diploids DNY11 and DNY26 are isogenic except that DNY11 is heterozygous for the *his4-lop* allele and DNY26 is heterozygous for the *his4-lopc* allele. DCB9 is isogenic with DNY26; all other diploids are isogenic with DNY11.

[b]Chi-square tests were performed using the numbers of aberrant and non-aberrant tetrads for DNY11 versus ER6, ER3, JDM1076, MD137, and MD138, and DNY26 versus DCB9. The p values for these six comparisons were ranked and the Benjamini and Hochberg (62) procedure was applied with an initial α value of 0.05. p values of less than 0.012 were considered significant. The comparisons with such p values were: ER6 and DNY11 ($p \leq 0.0001$), DCB9 and DNY26 ($p \leq 0.0001$), and JDM1076 and DNY11 ($p = 0.006$).

[c]Calculated using the standard equation (63). The DCB9 strain has a significantly ($p = 0.001$) elevated map distance compared to DNY26. All other alterations are statistically insignificant ($p \geq 0.05$).